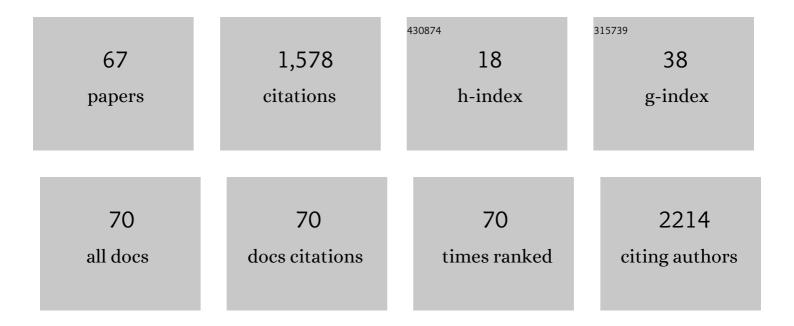
Felipe Caballero-Briones

List of Publications by Year in descending order

Source: https://exaly.com/author-pdf/9259502/publications.pdf Version: 2024-02-01



#	Article	lF	CITATIONS
1	Graphene oxide powders with different oxidation degree, prepared by synthesis variations of the Hummers method. Materials Chemistry and Physics, 2015, 153, 209-220.	4.0	516
2	Direct Observation of the Valence Band Edge by in Situ ECSTM-ECTS in p-Type Cu ₂ O Layers Prepared by Copper Anodization. Journal of Physical Chemistry C, 2009, 113, 1028-1036.	3.1	99
3	Growth of ordered anodic SnO ₂ nanochannel layers and their use for H ₂ gas sensing. Journal of Materials Chemistry A, 2014, 2, 915-920.	10.3	60
4	Study and improvement of aluminium doped ZnO thin films: Limits and advantages. Electrochimica Acta, 2013, 109, 117-124.	5.2	51
5	Effect of indium tin oxide substrate roughness on the morphology, structural and optical properties of CdS thin films. Applied Surface Science, 2000, 161, 340-346.	6.1	49
6	Structural and rheological changes of texturized mung bean protein induced by feed moisture during extrusion. Food Chemistry, 2021, 344, 128643.	8.2	49
7	Tin passivation in alkaline media: Formation of SnO microcrystals as hydroxyl etching product. Electrochimica Acta, 2013, 111, 837-845.	5.2	45
8	Evidence and analysis of parallel growth mechanisms in Cu2O films prepared by Cu anodization. Electrochimica Acta, 2010, 55, 4353-4358.	5.2	40
9	First stages of growth of CdS films on different substrates. Applied Surface Science, 1999, 148, 42-49.	6.1	34
10	Carbon-based radar absorbing materials: A critical review. Journal of Science: Advanced Materials and Devices, 2022, 7, 100454.	3.1	33
11	X-Ray photoelectron spectroscopy study of CdTe oxide films grown by rf sputtering with an Ar–NH3 plasma. Surface and Coatings Technology, 2002, 155, 16-20.	4.8	31
12	Experimental and DFT studies on the ultrasonic energy-assisted extraction of the phytochemicals of <i>Catharanthus roseus</i> as green corrosion inhibitors for mild steel in NaCl medium. RSC Advances, 2020, 10, 5399-5411.	3.6	31
13	Electrochemical and photocurrent characterization of polymer solar cells with improved performance after GO addition to the PEDOT:PSS hole transporting layer. Solar Energy, 2017, 146, 230-242.	6.1	25
14	Optical and structural evidence of the grain-boundary influence on the disorder of polycrystalline CdTe films. Applied Physics Letters, 1999, 74, 2957-2959.	3.3	23
15	Praseodymium-decorated graphene oxide as a corrosion inhibitor in acidic media for the magnesium AZ31 alloy. RSC Advances, 2018, 8, 34275-34286.	3.6	23
16	Chemical and phase composition of SnOx:F films grown by DC reactive sputtering. Surface and Coatings Technology, 2001, 148, 103-109.	4.8	22
17	CulnSe2 films prepared by three step pulsed electrodeposition. Deposition mechanisms, optical and photoelectrochemical studies. Electrochimica Acta, 2011, 56, 9556-9567.	5.2	22
18	Hybrid Carbon Nanochromium Composites Prepared from Chrome-Tanned Leather Shavings for Dye Adsorption. Water, Air, and Soil Pollution, 2019, 230, 1.	2.4	21

Felipe Caballero-Briones

#	Article	IF	CITATIONS
19	Experimental evidence of compositional mixture in CdTeO films grown by radio-frequency sputtering. Journal of Applied Physics, 1999, 86, 4688-4690.	2.5	19
20	Structure and mechanical properties of graphene oxide-reinforced polycarbonate. Materials Chemistry and Physics, 2021, 261, 124180.	4.0	19
21	Enhancement in as-grown CuInSe2 film microstructure by a three potential pulsed electrodeposition method. Electrochemistry Communications, 2010, 12, 1025-1029.	4.7	18
22	Disruption of the Chemical Environment and Electronic Structure in p-Type Cu ₂ O Films by Alkaline Doping. Journal of Physical Chemistry C, 2012, 116, 13524-13535.	3.1	18
23	Effect of calcination temperature on structure and thermoelectric properties of CuAlO2 powders. Journal of Materials Science, 2018, 53, 1646-1657.	3.7	18
24	Discharge diagnosis and controlled deposition of SnOx:F films by DC-reactive sputtering from a metallic tin target. Surface and Coatings Technology, 1999, 122, 136-142.	4.8	16
25	Phase tailored, potentiodynamically grown p-Cu2â^'xTe/Cu layers. Electrochemistry Communications, 2008, 10, 1684-1687.	4.7	16
26	The role of redox states and junctions in photocatalytic hydrogen generation of MoS2-TiO2-rGO and CeO2-Ce2Ti3O8.7-TiO2-rGO composites. Materials Science in Semiconductor Processing, 2020, 118, 105185.	4.0	16
27	Local atomic structure and analysis of secondary phases in non-stoichiometric Cu2ZnSnS4 using X-ray absorption fine structure spectroscopy. Journal of Alloys and Compounds, 2017, 714, 381-389.	5.5	15
28	Electricity generation from Nopal biogas effluent using a surface modified clay cup (cantarito) microbial fuel cell. Heliyon, 2019, 5, e01506.	3.2	15
29	Optical and electrical properties of graphene oxide and reduced graphene oxide films deposited onto glass and Ecoflex® substrates towards organic solar cells. Advanced Materials Letters, 2018, 9, 58-65.	0.6	15
30	Strain gradients in polycrystalline CdS thin films. Thin Solid Films, 2000, 373, 6-9.	1.8	14
31	Graphene oxide influence on selected properties of polymer fuel cells based on Nafion. International Journal of Hydrogen Energy, 2017, 42, 15359-15369.	7.1	14
32	A climatological estimate of incident solar energy in Tamaulipas, northeastern Mexico. Renewable Energy, 2013, 60, 293-301.	8.9	13
33	Neodymium-decorated graphene oxide as a corrosion barrier layer on Ti6Al4V alloy in acidic medium. RSC Advances, 2019, 9, 8537-8545.	3.6	13
34	Depth Profiling Study of the CdTe/CdS/ITO/Glass Heterostructure with AES and GIXRD. Physica Status Solidi (B): Basic Research, 2000, 220, 261-267.	1.5	12
35	X-ray study of tin oxide films obtained by reactive DC sputtering from a metallic tin target in pure oxygen plasma. Surface and Coatings Technology, 2007, 201, 4659-4665.	4.8	12
36	S diffusion at the CdTe/CdS interface grown by rf magnetron sputtering. Materials Letters, 1998, 37, 281-284.	2.6	10

#	Article	IF	CITATIONS
37	Phase control in selenium electrodeposition with bath temperature and deposition potential. Materials Research Express, 2019, 6, 066412.	1.6	9
38	One-step, low temperature synthesis of reduced graphene oxide decorated with ZnO nanocrystals using galvanized iron steel scrap. Materials Research Express, 2021, 8, 065010.	1.6	9
39	Structural analysis of Cd–Te–O films prepared by RF reactive sputtering. Journal of Non-Crystalline Solids, 2008, 354, 3756-3761.	3.1	8
40	Physical properties of transparent conducting Cd–Te–In–O thin films. Thin Solid Films, 2009, 518, 413-418.	1.8	8
41	Chemical Bonding and Electronic Structure in CdS/GO and CdSSe/GO Multilayer Films. Journal of Physical Chemistry C, 2019, 123, 13918-13924.	3.1	8
42	Effect of annealing temperature on the crystalline quality and phase transformation of Chemically Deposited CdSe films. Physica Status Solidi C: Current Topics in Solid State Physics, 2005, 2, 3742-3745.	0.8	7
43	COMPOSITION MIXTURE PROBABILISTIC MODEL IN THE FORMATION OF SEMICONDUCTOR MATERIALS OBTAINED BY RANDOM GROWTH TECHNIQUES. Modern Physics Letters B, 2001, 15, 643-646.	1.9	6
44	Influence of texture on the electrical properties of Al-doped ZnO films prepared by ultrasonic spray pyrolysis. Journal of Materials Science: Materials in Electronics, 2018, 29, 2016-2025.	2.2	6
45	Influence of pulse frequency on the morphology, structure and optical properties of ZnO films prepared by pulsed electrodeposition. Materials Research Express, 2019, 6, 086464.	1.6	6
46	Low resistance, high mobility reduced graphene oxide films prepared with commercial antioxidant supplements. Materials Letters, 2020, 276, 128176.	2.6	6
47	Chemical and microstructural study in radio frequency sputtered CdTe oxide films prepared at different N2O pressures. Oxygen incorporation and film resputtering. Thin Solid Films, 2008, 516, 8289-8294.	1.8	5
48	Influence of laser pulse regime on the structure and optical properties of TiO ₂ nanolayers. Materials Research Express, 2018, 5, 125022.	1.6	5
49	\$\${mathrm{{Cu}}_2mathrm{{ZnSnS}}_4}\$\$ thin films prepared with a Joule-heated graphite closed-space sulfurization system. Applied Physics A: Materials Science and Processing, 2019, 125, 1.	2.3	4
50	FTIR studies of the thermo-reversible sol–gel transition of a titanium butoxide solution modified by nitrate ions. Journal of Sol-Gel Science and Technology, 2021, 99, 315-325.	2.4	4
51	Deposit of AlN thin films by nitrogen reactive pulsed laser ablation using an Al target. Revista Mexicana De FÃsica, 2019, 65, 345-350.	0.4	4
52	Stoichiometry Calculation in BaxSr1â^'xTiO3 Solid Solution Thin Films, Prepared by RF Cosputtering, Using X-Ray Diffraction Peak Positions and Boltzmann Sigmoidal Modelling. Journal of Nanomaterials, 2017, 2017, 1-8.	2.7	3
53	Temperature–Power Simultaneous Effect on Physical Properties of BaxSr1â^'x TiO3 Thin Films Deposited by RF–Magnetron Cosputtering for 0 ≤ ≤. Coatings, 2018, 8, 362.	2.6	3
54	Formation of magnetic nanoscrolls and nanoribbons in iron oxide-decorated graphene oxide. Materials Letters, 2022, 309, 131321.	2.6	3

Felipe Caballero-Briones

#	Article	IF	CITATIONS
55	Structural damage in graphene oxide coatings onto Nb substrates upon laser irradiation. Surface and Coatings Technology, 2022, 431, 128013.	4.8	3
56	Tunable, Wideband X-Band Microwave Absorbers Using Variable Chessboard Surfaces. IEEE Letters on EMC Practice and Applications, 2022, 4, 44-46.	1.1	3
57	Cesium-decorated reduced graphene oxide for photocatalytic hydrogen generation. Materials Letters, 2022, 314, 131864.	2.6	3
58	Automated Instrument for the Deposition of Thin Films Using Successive Ionic Layer Adsorption and Reaction. Processes, 2022, 10, 492.	2.8	3
59	CHEMICAL COMPOSITION AND CRYSTALLINE PHASES IN F-DOPED TIN OXIDE FILMS GROWN BY DC REACTIVE SPUTTERING. Modern Physics Letters B, 2001, 15, 634-638.	1.9	2
60	Chemical bath deposited CdS films using magnetic treated solutions. Physica Status Solidi (B): Basic Research, 2005, 242, 1933-1936.	1.5	2
61	Calcium content and speciation in alkaline-cooked corn studied byÂsynchrotron Ca K-edge X-ray absorption spectroscopy. Journal of Cereal Science, 2014, 60, 7-10.	3.7	2
62	Method to estimate crystallinity in nixtamalized corn pericarp from sequential extractions and X-ray diffraction. Journal of Cereal Science, 2015, 64, 11-15.	3.7	2
63	Photoluminescence Response in Carbon Films Deposited by Pulsed Laser Deposition onto GaAs Substrates at Low Vacuum. Journal of Nanotechnology, 2016, 2016, 1-6.	3.4	2
64	Local Electrical Response in Alkaline-Doped Electrodeposited CuInSe2/Cu Films. Coatings, 2016, 6, 71.	2.6	2
65	Structure, morphology, and local photoelectrical characterization of PbS films grown by SILAR. Materials Letters, 2022, 314, 131844.	2.6	2
66	Local hardening of Raman phonons in BaxSr1â^'xTiO3 thin films deposited by r.f. sputtering. Materials Research Express, 2020, 7, 046402.	1.6	1
67	Two Dimensional-Based Materials for Photocatalysis Applications. Environmental Chemistry for A Sustainable World, 2020, , 275-293.	0.5	0